

Synthesis of PVA/Fe₃O₄@SiO₂@CPS@SID@Ni as novel magnetic fibrous composite polymer nanostructures and evaluation of anticancer and antimicrobial activity

Mohammadreza Moghaddam-manesh (✉ mrm.manesh@gmail.com)

standard research institute <https://orcid.org/0000-0002-0590-9622>

Ghasem Sargazi

Mehdi Roohani

Nooshin Gholipour Zanjani

Mahroo Khaleghi

Sara Hosseinzadegan

Research Article

Keywords: PVA/Fe₃O₄, fibrous composite polymer, Magnetic, [1,3]dithiine, Anticancer activity, Antimicrobial activity

Posted Date: April 14th, 2022

DOI: <https://doi.org/10.21203/rs.3.rs-1524316/v1>

License:   This work is licensed under a Creative Commons Attribution 4.0 International License. [Read Full License](#)

Abstract

Novel PVA/Fe₃O₄@SiO₂@CPS@SID@Ni magnetic fibrous composite polymer (PVA/MFCP) were synthesized and its structure by Scanning Electron Microscopy (SEM), Fourier Transform Infrared spectroscopy (FT-IR), X-Ray Diffraction (XRD), Vibrating Sample Magnetometer (VSM), N₂ adsorption/desorption isotherms and thermal behavior were confirmed. Anticancer properties of synthetic PVA/Fe₃O₄@SiO₂@CPS@SID@Ni (MFCP) were evaluated by MTT method on MCF-7 breast cancer cells and IC₅₀ 119 µg/ml was observed at 48 hours. Antibacterial and antifungal properties of the synthesized MFCP nanostructures based on Minimum Inhibitory Concentration (MIC), Minimum Bactericidal Concentration (MBC) and Minimum Fungicidal Concentration (MFC) were tested and the results proved in some cases have better effect than commercial drugs.

Introduction

Nowadays, the synthesis of magnetic nanoparticles get an importance due to their various applications and their activity as an environmentally friendly catalysts in the synthesis of organic compounds [1–6]. Applications such as adsorption of dyes [7], data storage and solar cells from magnetic nanoparticles have been reported. In medicine, applications such as biomolecular sensors and drug delivery of magnetic nanoparticles have been Identified [2].

[1, 3] Dithiines are heterocyclic compounds with 2 sulfur atoms with different biological properties [8–12]. Antibacterial and antifungal activity of magnetic nanoparticles containing this heterocyclic have been studied and acceptable biological effects have been observed [13, 14].

Besides, the magnetic nanoparticles was used in the synthesis of PVA/cellulose whiskers nanocomposite [15, 16]. One of the most practical nanostructures are nanofibers, which have found many industrial applications due to their interesting properties. Applications of nanofibers in biological and medical fields include food packaging, enzyme stabilization, weaving engineering, and wound dressing [17]. Preparation of antimicrobial nanofiber coating has been considered by researchers due to its many medical and biological applications [18, 19]. The antimicrobial nanofilament dressings could prevent wound infection and accelerate wound healing and thus reduces the duration of treatment. The reports on the application of antimicrobial nanofibers using polymer compounds and different plant extracts could confirm this property [20].

As we know cancer is one of the leading causes of death for millions of people worldwide, the use of traditional drugs to treat cancer has limitations such as poor pharmacokinetics, poor biological distribution and adverse side effects, and chemotherapy as a common method of treatment of the cancer has disadvantages such as low therapeutic efficiency in the treatment process and side effects on normal cells, so scientists are trying to use new methods and the use of nanoparticles in the treatment of cancer. Nanostructures such as graphene oxide, metal-organic frameworks and magnetite have been reported in the treatment of cancer based on popular drug delivery systems [21, 22].

In this study, novel fibrous composite polymer containing [1, 3]dithiines magnetic nanoparticles (PVA/MFCP) were synthesized and their antimicrobial and anticancer activities were evaluated.

Experimental Section

General

All reagents, solvents and drugs were purchased from Sigma-Aldrich and Merck. The SEM image of nanoparticles (scanning electron microscopic) was studied using a Hitachi S4160 instrument. The FT-IR spectra were recorded on Bruker Tensor 27 FT-IR spectrometer by using KBr pellets. Bruker D8 X-ray diffractometer with Cu-K α radiation ($\lambda = 1.5418 \text{ \AA}$) in the range of 10–70° and the scanning rate of 1.5°/min was conducted for X-ray diffraction (XRD) analysis of nanoparticles. Magnetic measurements were carried out at room temperature by using LBKFB from Meghnatis Daghigh Kavir Company. In anticancer activity, the absorbance at 570 nm was read utilizing a BioTek Instruments spectrophotometer. In antimicrobial activity, the concentrations of bacterial, fungal suspensions were prepared by using Jenway 6405 UV–Vis spectrophotometer.

Synthesis of Fe₃O₄@SiO₂@CPS@SID@Ni

Spiro[indoline-3,40-[1,3]dithiine]@Ni (NO₃)₂ supported on Fe₃O₄@SiO₂@CPS (Fe₃O₄@SiO₂@CPS@SID@Ni) was synthesized according to our previously reported method [14].

Synthesis of PVA/Fe₃O₄@SiO₂@CPS@SID@Ni MFCP nanostructures (PVA/MFCP)

PVA/Fe₃O₄@SiO₂@CPS@SID@Ni were synthesized according to previously reported methods [23, 24]; briefly, 10 mg Fe₃O₄@SiO₂@CPS@SID@Ni was dissolved in 25 ml of distilled water. In another container, 4 mg PVA was dissolved in 20 mL of n-hexane. Then two prepared solution mixed together and was stirred at 80 °C for 20 min. After that, by spinning distance of 22 cm, voltage of 28 kV and a flow rate of 0.4 mL/h as optimum conditions of the electrospinning method, PVA/Fe₃O₄@SiO₂@CPS@SID@Ni (PVA/MFCP) were synthesized.

Anticancer activity

Anticancer activity of PVA/MFCP nanostructures on MCF-7 breast cancer cells and cell viability assay, according to previously reported methods and MTT method were tested. Concentrations of 5, 10, 20, 40, 80, 120 and 200 $\mu\text{g/ml}$ from PVA/MFCP nanostructures at 24 and 48 hours in density of 1.2×10^4 (cells/well) were treated [25].

Antimicrobial activity

Antibacterial and antifungal activity of PVA/MFCP nanostructures on Gram-negative pathogenic strains, Gram- positive pathogenic bacteria and fungi based on Minimum Inhibitory Concentration (MIC), Minimum Bactericidal Concentration (MBC) and Minimum Fungicidal Concentration (MFC) values were tested. In

antimicrobial activity, all tests were repeated three times and the mean values of the test results were reported.

MIC TEST

According to the CLSI guidelines M07-A9 and M27-A2 and previously reported methods, broth microdilution susceptibility to MIC test of PVA/MFCP nanostructures were evaluated [7, 26].

MBC and MFC TESTS

The Time-kill test was done to determine MBC and MFC values, according to the CLSI guideline M26-A and previously reported methods [7, 26].

Results And Discussion

Synthesis and characterization of PVA/Fe₃O₄@SiO₂@CPS@SID@Ni MFCP (PVA/MFCP) nanostructures

Identification and characterization of PVA/MFCP (Fig. 1) were performed by using scanning electron microscopy (SEM), infrared spectroscopy (FT-IR), X-ray diffraction (XRD), vibrating sample magnetometer (VSM), N₂ adsorption/desorption isotherms and thermal behaviour.

According to our previous reports, structure of Fe₃O₄@SiO₂@CPS@SID@Ni was validated through spectral data (Fig. 2) such as SEM, FT-IR, XRD, EDX and VSM [14]. In this work, SEM, FT-IR, XRD and VSM spectral data of PVA/MFCP nanostructures was compared with our previous reports.

Previous reports in SEM image of Fe₃O₄@SiO₂@CPS@SID@Ni (Fig. 3-I) suggest that its particle size is in the nanoscale range with uniform morphology [14], in the final structure (PVA/MFCP) the morphology was preserved (Fig. 3-II) which proves that the electrospinning procedure were optimal conditions and the PVA/MFCP nanostructures was in the nanoscale range.

All peaks of the proposed structure were observed in the FT-IR spectrum of PVA/MFCP nanostructures (Fig. 4-II). Comparison spectra of Fe₃O₄@SiO₂@CPS@SID@Ni [14] and PVA/MFCP nanostructures showed that in addition to peaks Ni-N, Fe-O, Si-O, C = C, C = O, CN, C-H and N-H, there are peaks related to Ni-O and O-H in areas 700 cm⁻¹ and 3200 cm⁻¹, respectively, in spectrum of PVA/Fe₃O₄@SiO₂@CPS@SID@Ni.

The XRD pattern of PVA/MFCP nanostructures was similar to the XRD pattern of Fe₃O₄@SiO₂@CPS@SID@Ni and in positions of 2θ angles at 30.2, 35.69, 43.5, 53.75, 57.6 and 63.8 due to the standard XRD pattern of crystalline cubic spinel Fe₃O₄ nanoparticles were shown (Fig. 5) [3, 14].

According to our previous report, vibrating sample magnetometer related to structure Fe₃O₄@SiO₂@CPS@SID@Ni, 23.8 emu g⁻¹ was observed [14], vibrating sample magnetometer related to

PVA/ MFCP, 7.6 emu g^{-1} was observed (Fig. 6), decreasing the amount of VSM proves the structure of the proposed product.

According to N_2 adsorption/desorption isotherms of synthesized material under optimal conditions in Fig. 7, the adsorption/ desorption isotherms of both sample are similar to first type of classical isotherms which confirms microporous distribution of products [27, 28]. Based on data obtained from BET technique, PVA/MFCP nanostructures have more surface area than PVA/ $\text{Fe}_3\text{O}_4@SiO_2$ ($1170 \text{ m}^2/\text{g}$ compared to $680 \text{ m}^2/\text{g}$). It means that incorporation of the nanostructures in core-shell composite network could enhance the surface area of the final products.

Thermal behavior of $\text{Fe}_3\text{O}_4@SiO_2$ and PVA/MFCP nanostructures synthesized under optimal conditions are showed in Fig. 8. According to this **Fig**, the samples have thermal behavior including evaporation the solvent (near $100 \text{ }^\circ\text{C}$), destruction trapping solvent (around 140°C) and disintegrate the main structure. The data obtained from this curve showed that PVA/MFCP nanostructures have higher thermal stability ($235 \text{ }^\circ\text{C}$ than $187 \text{ }^\circ\text{C}$). As an important result, synthesis of nanostructures with desirable components could enhance the thermal stability of compound with high degree. This product can be used in different area such as novel catalyst with high thermal stability [29, 30].

Anticancer properties

Anticancer activity of PVA/MFCP nanostructures on MCF-7 breast cancer cells in 24 and 48 hours at a concentration of $200 \text{ }\mu\text{g}/\text{mL}$ showed the maximum effect and were about 40% and 32% than control, respectively (Fig. 9).

IC_{50} values of PVA/ $\text{Fe}_3\text{O}_4@SiO_2@CPS@SID@Ni$ MFCP nanostructures at 24h and 48h were calculated as $152 \text{ }\mu\text{g}/\text{mL}$ and $119 \text{ }\mu\text{g}/\text{mL}$, respectively.

From the results of anticancer activity, it can be concluded that the effectiveness of PVA/ $\text{Fe}_3\text{O}_4@SiO_2@CPS@SID@Ni$ MFCP nanostructures depends on time and concentration.

Antimicrobial properties

According to our previous report, the antimicrobial properties of magnetic nanoparticles were investigated on *Fusarium oxysporum* (PTCC 5115) as fungi and Gram-positive pathogenic strains including *Staphylococcus aureus* (PTCC 1189) and *Rhodococcus equi* (PTCC 1633), Gram-negative pathogenic strains including *Proteus mirabilis* (PTCC 1776), *Escherichia coli* (PTCC 1399) and *Salmonella enterica* subsp. *enterica* (PTCC 1709) that were prepared from the Persian Type Culture Collection (PTCC), Tehran, Iran. In this study, the antimicrobial properties of PVA/ $\text{Fe}_3\text{O}_4@SiO_2@CPS@SID@Ni$ MFCP nanostructures on the mentioned strains were evaluated and the results were presented in Table 1.

Table 1
Antimicrobial activities of PVA/Fe₃O₄@SiO₂@CPS@SID@Ni MFCP

Product / Antibiotics	Fungi		gram- positive				gram- negative					
	5115		1189		1633		1776		1399		1709	
	MIC	MFC	MIC	MBC	MIC	MBC	MIC	MBC	MIC	MBC	MIC	MBC
P/MFCP	256	256	128	256	8	32	16	32	8	16	32	128
SID MNPs ^[14]	128	256	256	512	16	32	16	32	8	16	64	128
Drug a ^[14]	-	-	0.5	1	1	4	0.5	2	4	8	4	8
Drug b ^[14]	32	64	8	16	8	16	16	16	-	-	8	16
P/MFCP: PVA/Fe ₃ O ₄ @SiO ₂ @CPS@SID@Ni MFCP nanostructures as novel magnetic fibrous composite polymer												
SID MNPs: Fe ₃ O ₄ @SiO ₂ @CPS@SID@Ni												
MIC, MBC and MFC Values reported as µg/mL												
For fungi; Drug a: Tolnaftate, Drug b: Terbinafine; For bactria; Drug a: Gentamicin, Drug b: Penicillin												

As shown in the Table 1, antimicrobial activity of PVA/Fe₃O₄@SiO₂@CPS@SID@Ni MFCP nanostructures and Fe₃O₄@SiO₂@CPS@SID@Ni based on minimum inhibitory concentration (MIC), minimum bactericidal concentration (MBC) and minimum fungicidal concentration (MFC) were evaluated and have been compared with Tolnaftate, Terbinafine as commercial antifungal drugs and Gentamicin, Penicillin, as commercial antibacterial drugs.

Based on MBC and MFC Values, the results of antimicrobial activity from PVA/Fe₃O₄@SiO₂@CPS@SID@Ni MFCP nanostructures was very similar to Fe₃O₄@SiO₂@CPS@SID@Ni.

The results showed that Tolnaftate as commercial antifungal drug did not effect on *Fusarium oxysporum*, but PVA/Fe₃O₄@SiO₂@CPS@SID@Ni MFCP nanostructures and Fe₃O₄@SiO₂@CPS@SID@Ni showed MFC 256 µg/mL in addition, Penicillin's commercial drug did not effect on *Escherichia coli*, but PVA/Fe₃O₄@SiO₂@CPS@SID@Ni MFCP nanostructures and Fe₃O₄@SiO₂@CPS@SID@Ni with MBC 16 µg/mL showed acceptable effects.

Conclusion

In this research, PVA/Fe₃O₄@SiO₂@CPS@SID@Ni as a novel magnetic fibrous composite polymer were synthesized. The structure was evaluated by scanning electron microscopy (SEM), infrared spectroscopy (FT-IR), X-ray diffraction (XRD), vibrating sample magnetometer (VSM), N₂ adsorption/desorption isotherms and thermal behavior, its anti-cancer and antimicrobial properties were investigated. The anti-cancer properties were evaluated using MTT method on MCF-7 breast cancer cells and after 48 hours the

maximum effect was about 32% than control and IC_{50} 119 $\mu\text{g/ml}$ were calculated. Antibacterial and antifungal properties of PVA/ $\text{Fe}_3\text{O}_4@SiO_2@CPS@SID@Ni$ magnetic fibrous composite polymer on gram-positive strains and gram-negative strains and fungal strains were evaluated and in some cases higher effects than commercial drugs were observed.

Declarations

Authors are required to disclose financial or non-financial interests that are directly or indirectly related to the work submitted for publication.

References

1. L. Shiri, L. Heidari, M. Kazemi: Magnetic Fe_3O_4 nanoparticles supported imine/Thiophene-nickel (II) complex (2018) A new and highly active heterogeneous catalyst for the synthesis of polyhydroquinolines and 2, 3-dihydroquinazoline-4 (1H)-ones. *Applied Organometallic Chemistry* **32**(1):e3943
2. S. Sajjadifar, Z. Gheisarzadeh, Isatin- SO_3H coated on amino propyl modified magnetic nanoparticles ($\text{Fe}_3\text{O}_4@APTES@isatin-\text{SO}_3\text{H}$) as a recyclable magnetic nanoparticle for the simple and rapid synthesis of pyrano [2, 3-d] pyrimidines derivatives. *Appl. Organomet. Chem.* **33**(1), e4602 (2019)
3. T. Tamoradi, M. Ghadermazi, A. Ghorbani-Choghamarani, Ni (II)-Adenine complex coated Fe_3O_4 nanoparticles as high reusable nanocatalyst for the synthesis of polyhydroquinoline derivatives and oxidation reactions. *Appl. Organomet. Chem.* **32**(1), e3974 (2018)
4. M.A. Zolfigol, M. Safaiee, N. Bahrami-Nejad, Dendrimeric magnetic nanoparticle cores with Co-phthalocyanine tags and their application in the synthesis of tetrahydrobenzo [b] pyran derivatives. *New J. Chem.* **40**(6), 5071–5079 (2016)
5. S. Hosseinzadegan, N. Hazeri, M.T. Maghsoodlou, Synthesis of novel thiazolo [3, 2-a] chromeno [4, 3-d] pyrimidine-6 (7H)-ones by bioactive $\text{Fe}_3\text{O}_4@gly@thiophen@Cu(NO_3)_2$ as reusable magnetic nanocatalyst. *Appl. Organomet. Chem.* **34**(9), e5797 (2020)
6. S.M. Mousavifar, H. Kefayati, S. Shariati, $\text{Fe}_3\text{O}_4@Propylsilane@Histidine[HSO_4^-]$ magnetic nanocatalysts: Synthesis, characterization and catalytic application for highly efficient synthesis of xanthene derivatives. *Appl. Organomet. Chem.* **32**(4), e4242 (2018)
7. S. Hosseinzadegan, N. Hazeri, M.T. Maghsoodlou, M. Moghaddam-Manesh, M. Shirzaei, Synthesis and evaluation of biological activity of novel chromeno [4, 3-b] quinolin-6-one derivatives by SO_3H -tryptamine supported on $\text{Fe}_3\text{O}_4@SiO_2@CPS$ as recyclable and bioactive magnetic nanocatalyst. *J. Iran. Chem. Soc.* **17**(12), 3271–3284 (2020)
8. A. Kamel, M. Saleh, Recent studies on the chemistry and biological activities of the organosulfur compounds of garlic (*Allium sativum*). *Stud. Nat. Prod. Chem.* **23**, 455–485 (2000)
9. F. Zentz, R. Labia, D. Sirot, O. Faure, R. Grillot, A. Valla, Syntheses, in vitro antibacterial and antifungal activities of a series of N-alkyl, 1, 4-dithiines. *Il Farmaco* **60**(11–12), 944–947 (2005)

10. A. Bielenica, J. Kossakowski, M. Struga, I. Dybała, P. La Colla, E. Tamburini, R. Loddo, Biological evaluation of novel 1, 4-dithiine derivatives as potential antimicrobial agents. *Med. Chem. Res.* **20**(8), 1411–1420 (2011)
11. E. Block, S. Ahmad, M.K. Jain, R.W. Crecely, R. Apitz-Castro, M.R. Cruz, The chemistry of alkyl thiosulfate esters. 8.(E, Z)-Ajoene (1984) a potent antithrombotic agent from garlic. *Journal of the American Chemical Society* **106**(26):8295–8296
12. R. Apitz-Castro, S. Cabrera, M. Cruz, E. Ledezma, M. Jain, Effects of garlic extract and of three pure components isolated from it on human platelet aggregation, arachidonate metabolism, release reaction and platelet ultrastructure. *Thromb. Res.* **32**(2), 155–169 (1983)
13. M. Moghaddam-Manesh, E. Sheikhhosseini, D. Ghazanfari, M. Akhgar (2020) Synthesis of novel 2-oxospiro [indoline-3, 4'-[1, 3] dithiine]-5'-carbonitrile derivatives by new spiro [indoline-3, 4'-[1, 3] dithiine]@ Cu (NO₃)₂ supported on Fe₃O₄@ gly@ CE MNPs as efficient catalyst and evaluation of biological activity. *Bioorg. Chem.* **98**:103751
14. M. Moghaddam-Manesh, D. Ghazanfari, E. Sheikhhosseini, M. Akhgar, Synthesis of bioactive magnetic nanoparticles spiro [indoline-3, 4'-[1, 3] dithiine]@ Ni (NO₃)₂ supported on Fe₃O₄@ SiO₂@ CPS as reusable nanocatalyst for the synthesis of functionalized 3, 4-dihydro-2H-pyran. *Appl. Organomet. Chem.* **34**(4), e5543 (2020)
15. M. Roohani, M. Shabani, B. Kord, M. Hajibeygi, H.A. Khonakdar, New functional Fe₃O₄ nanoparticles utilizing as adjuvant in the green PVA/cellulose whiskers nanocomposite. *Thermochim. Acta* **635**, 17–25 (2016)
16. C.W. Irvin, C.C. Satam, J.C. Meredith, M.L. Shofner, Mechanical reinforcement and thermal properties of PVA tricomponent nanocomposites with chitin nanofibers and cellulose nanocrystals. *Compos. Part A: Appl. Sci. Manufac.* **116**, 147–157 (2019)
17. R. Sridhar, J. Venugopal, S. Sundarrajan, R. Ravichandran, B. Ramalingam, S. Ramakrishna, Electrospun nanofibers for pharmaceutical and medical applications. *J. Drug Deliv. Sci. Technol.* **21**(6), 451–468 (2011)
18. N. Eghbalifam, S.A. Shojaosadati, S. Hashemi-Najafabadi, A.C. Khorasani, Synthesis and characterization of antimicrobial wound dressing material based on silver nanoparticles loaded gum Arabic nanofibers. *Int. J. Biol. Macromol.* **155**, 119–130 (2020)
19. M.M. Mahmud, S. Zaman, A. Perveen, R.A. Jahan, M.F. Islam, M.T. Arafat, Controlled release of curcumin from electrospun fiber mats with antibacterial activity. *J. Drug Deliv. Sci. Technol.* **55**, 101386 (2020)
20. W. Zhang, S. Ronca, E. Mele, Electrospun nanofibres containing antimicrobial plant extracts. *Nanomaterials* **7**(2), 42 (2017)
21. L.-L. Sun, Y.-H. Li, H. Shi, A ketone functionalized Gd (III)-MOF with low cytotoxicity for anti-cancer drug delivery and inhibiting human liver cancer cells. *J. Cluster Sci.* **30**(1), 251–258 (2019)
22. M. Pooresmaeil, H. Namazi, Facile preparation of pH-sensitive chitosan microspheres for delivery of curcumin; characterization, drug release kinetics and evaluation of anticancer activity. *Int. J. Biol. Macromol.* **162**, 501–511 (2020)

23. G. Sargazi, A.K. Ebrahimi, D. Afzali, A. Badoei-dalfard, S. Malekabadi, Z. Karami, Fabrication of PVA/ZnO fibrous composite polymer as a novel sorbent for arsenic removal: design and a systematic study. *Polym. Bull.* **76**(11), 5661–5682 (2019)
24. O. Azizabadi, F. Akbarzadeh, G. Sargazi, N.P.S. Chauhan, Preparation of a Novel Ti-metal Organic Framework Porous Nanofiber Polymer as an Efficient Dental Nano-coating: Physicochemical and Mechanical Properties. *Polymer-Plastics Technol. Mater.* **60**(7), 734–743 (2021)
25. M. Moghaddam-Manesh, S. Hosseinzadegan (2021) Introducing new method for the synthesis of polycyclic compounds containing [1, 3] dithiine derivatives, with anticancer and antibacterial activities against common bacterial strains between aquatic and human. *Journal of Heterocyclic Chemistry* 2021
26. M. Zeraati, M. Moghaddam-Manesh, S. Khodamoradi, S. Hosseinzadegan, A. Golpayegani, N.P.S. Chauhan, G. Sargazi, Ultrasonic assisted reverse micelle synthesis of a novel Zn-metal organic framework as an efficient candidate for antimicrobial activities. *J. Mol. Struct.* **1247**, 131315 (2022)
27. G. Sargazi, D. Afzali, A. Mostafavi, H. Kazemian, A novel composite derived from a metal organic framework immobilized within electrospun nanofibrous polymers: An efficient methane adsorbent. *Appl. Organomet. Chem.* **34**(3), e5448 (2020)
28. M. Kaykhaii, S.H. Hashemi, F. Andarz, A. Piri, G. Sargazi, G. Boczkaj, Chromium-based metal organic framework for pipette tip micro-solid phase extraction: an effective approach for determination of methyl and propyl parabens in wastewater and shampoo samples. *BMC Chem.* **15**(1), 1–12 (2021)
29. H. Deng, S. Kang, C. Wang, H. He, C. Zhang, Palladium supported on low-surface-area fiber-based materials for catalytic oxidation of volatile organic compounds. *Chem. Eng. J.* **348**, 361–369 (2018)
30. S. Abbas, H. Lee, J. Hwang, A. Mehmood, H.-J. Shin, S. Mehboob, J.-Y. Lee, H.Y. Ha, A novel approach for forming carbon nanorods on the surface of carbon felt electrode by catalytic etching for high-performance vanadium redox flow battery. *Carbon* **128**, 31–37 (2018)

Figures

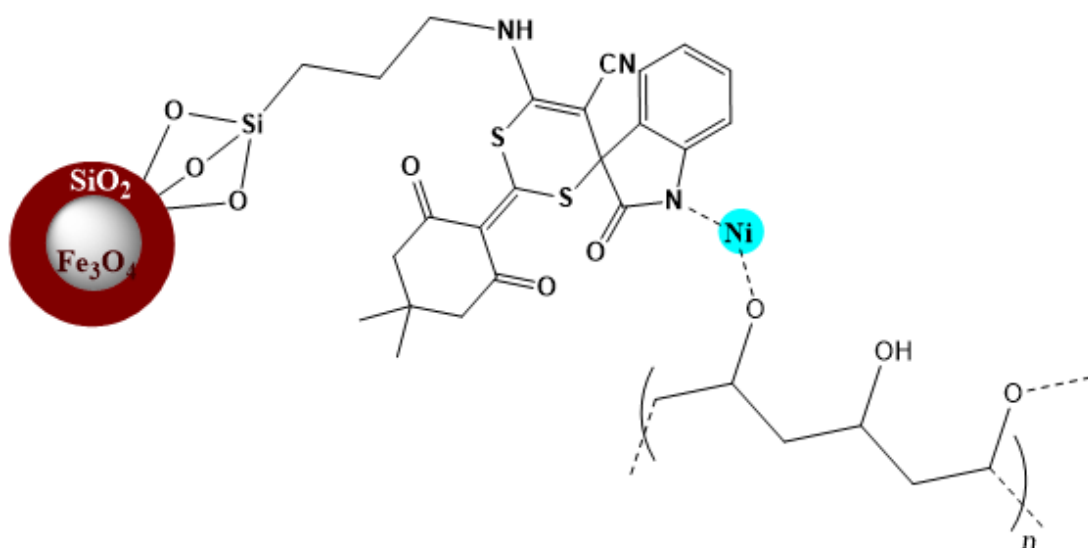


Figure 1

Structure of synthesized PVA/MFCP nanostructures

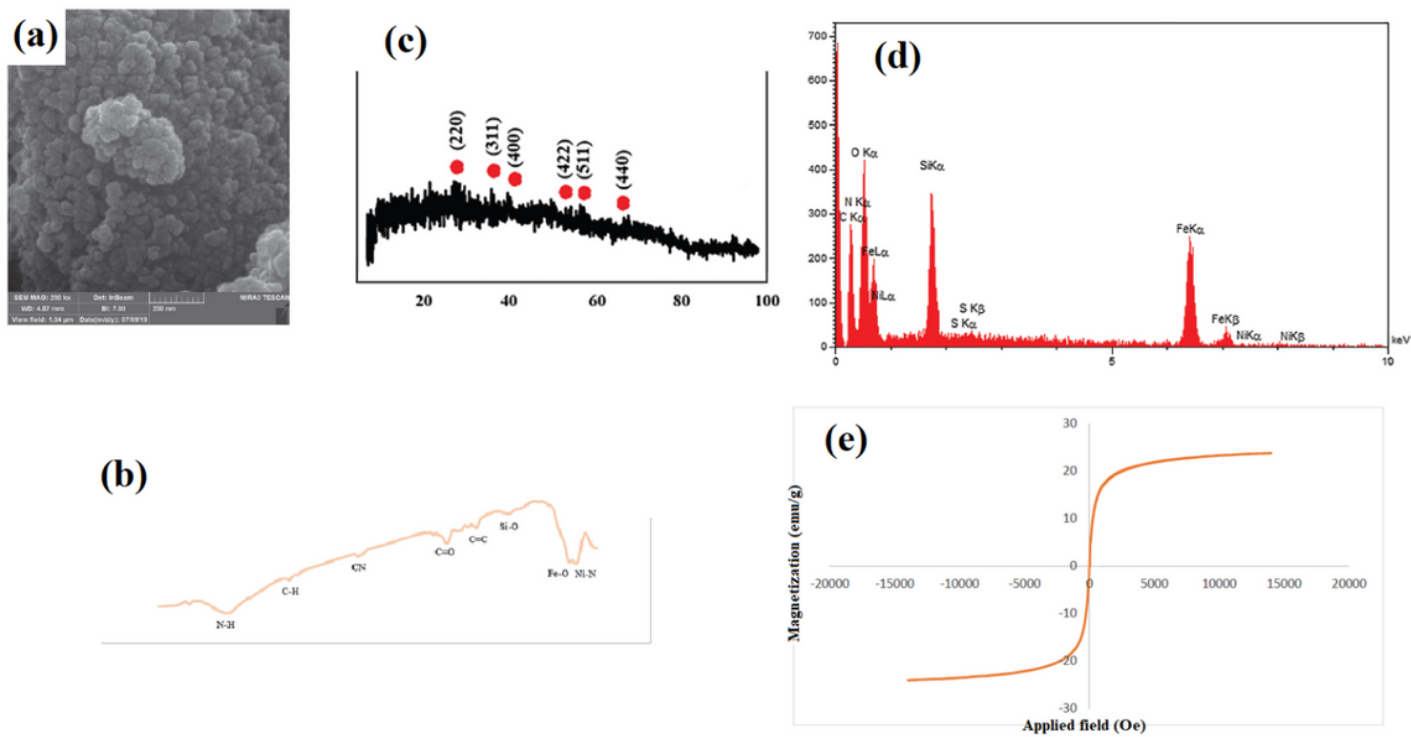


Figure 2

SEM (a), FT-IR (b), XRD (c), EDX (d) and VSM (e) of $\text{Fe}_3\text{O}_4@\text{SiO}_2@\text{CPS}@\text{SID}@\text{Ni}$

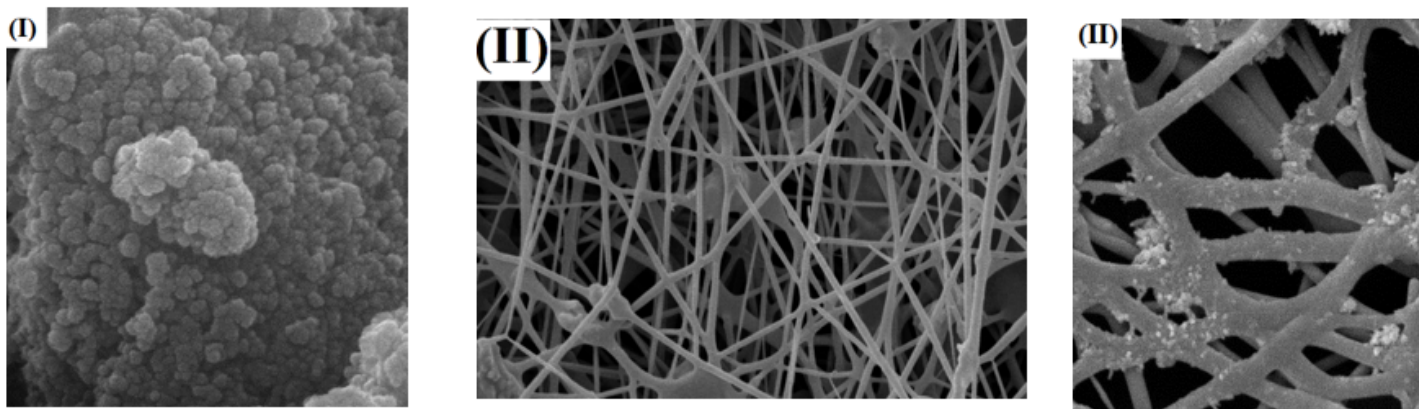


Figure 3

SEM image of $\text{Fe}_3\text{O}_4@\text{SiO}_2@\text{CPS}@\text{SID}@\text{Ni}$ (I) and PVA/MFCP nanostructures (II)

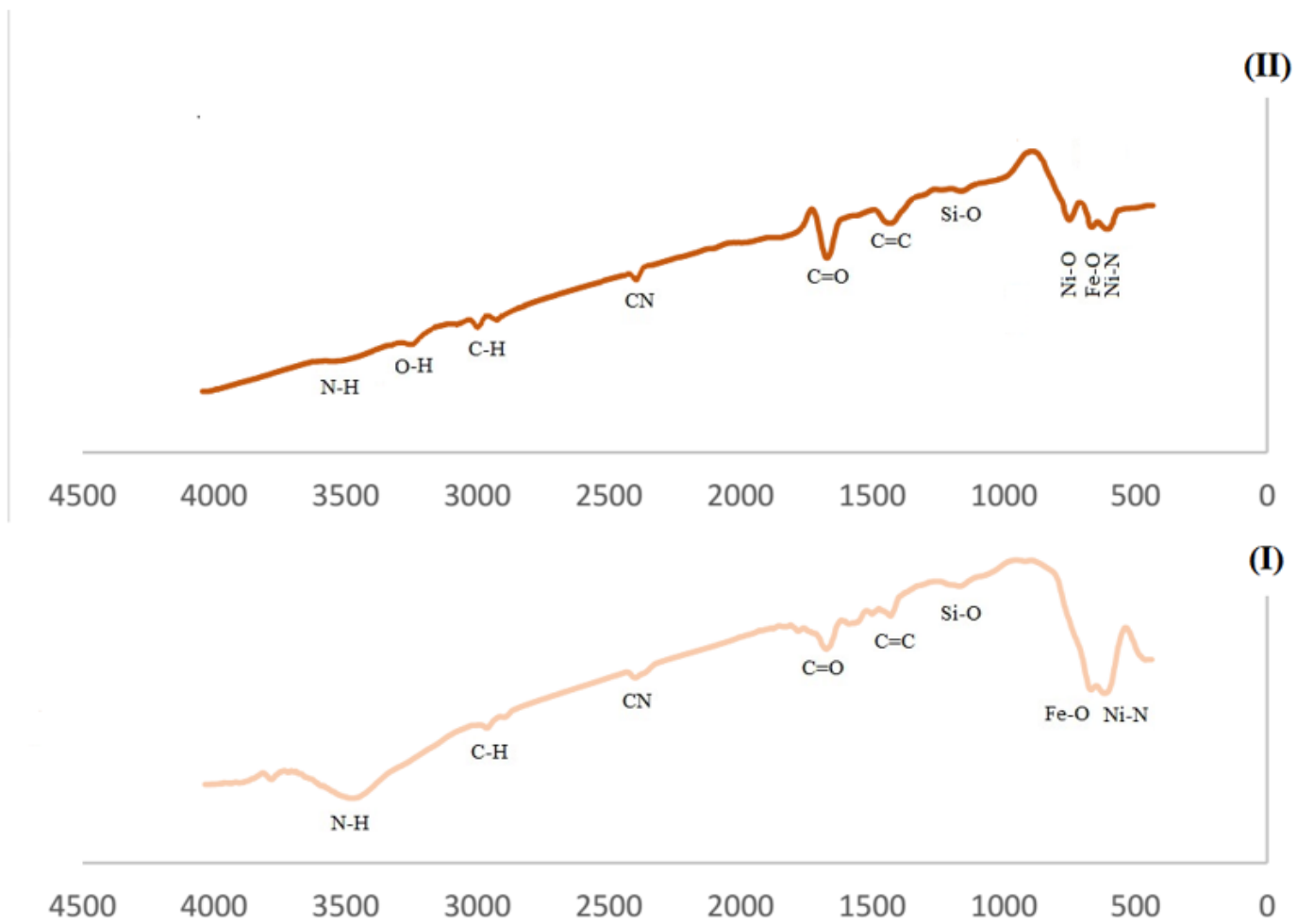


Figure 4

FT-IR spectrum of Fe₃O₄@SiO₂@CPS@SID@Ni (I) and PVA/MFCP nanostructures (II)

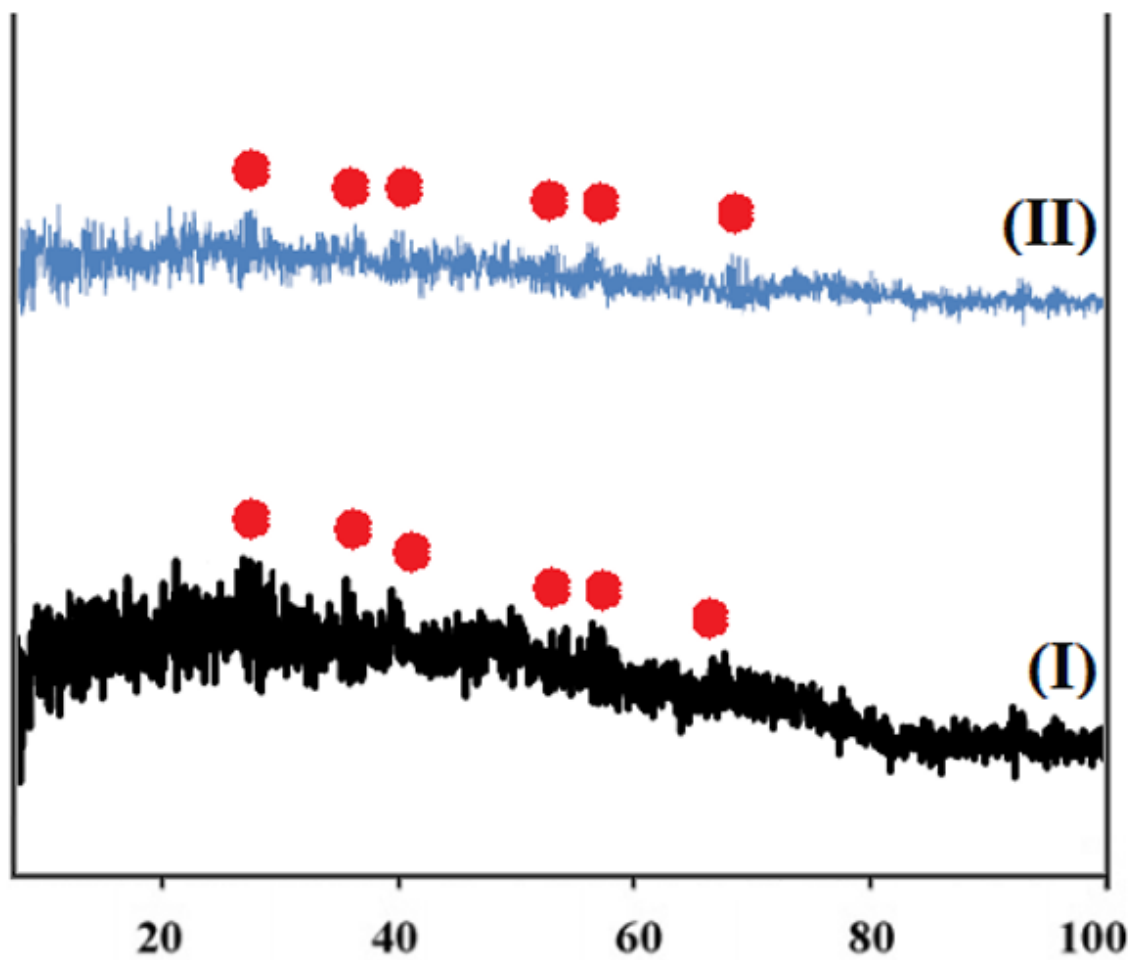


Figure 5

XRD pattern of Fe₃O₄@SiO₂@CPS@SID@Ni (I) and PVA/MFCP nanostructures (II)

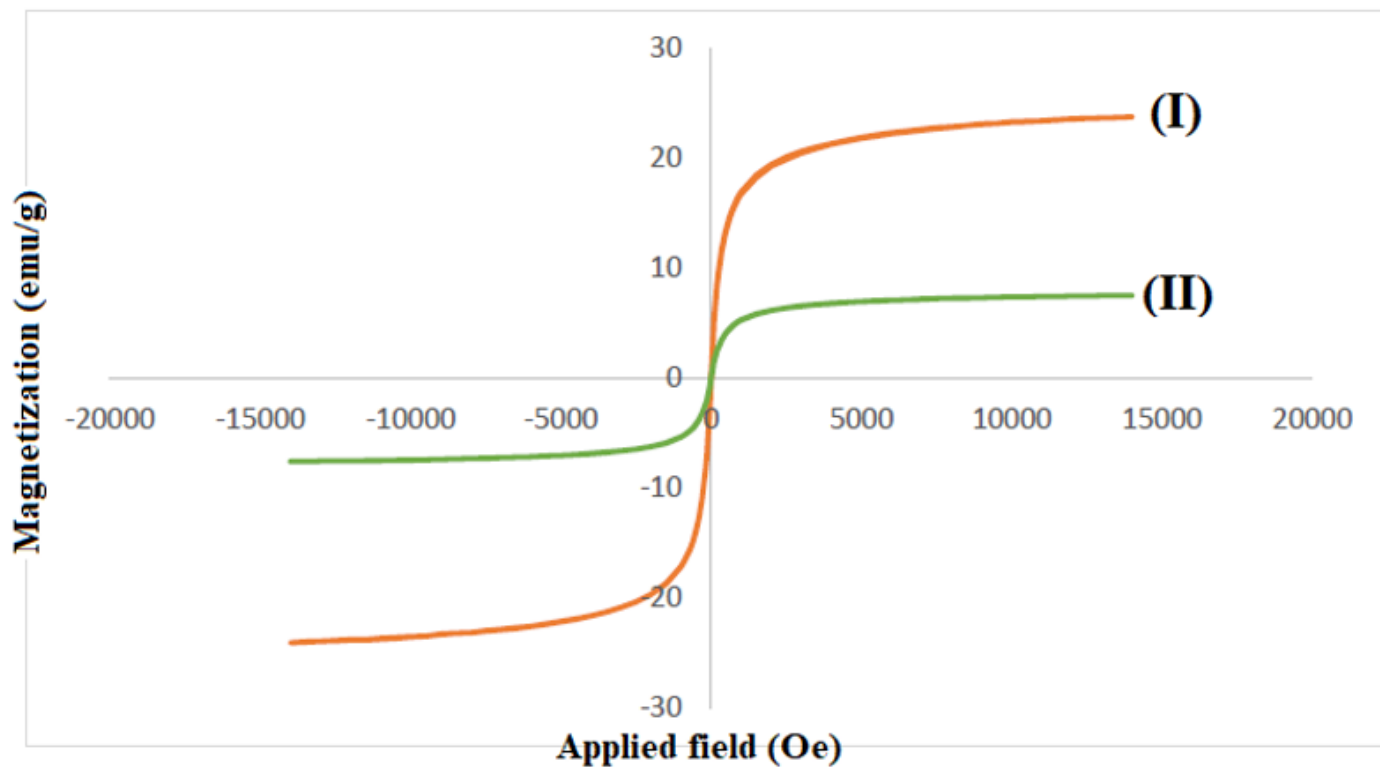


Figure 6

VSM curve of $\text{Fe}_3\text{O}_4@SiO_2@CPS@SID@Ni$ (I) and PVA/MFCP nanostructures (II)

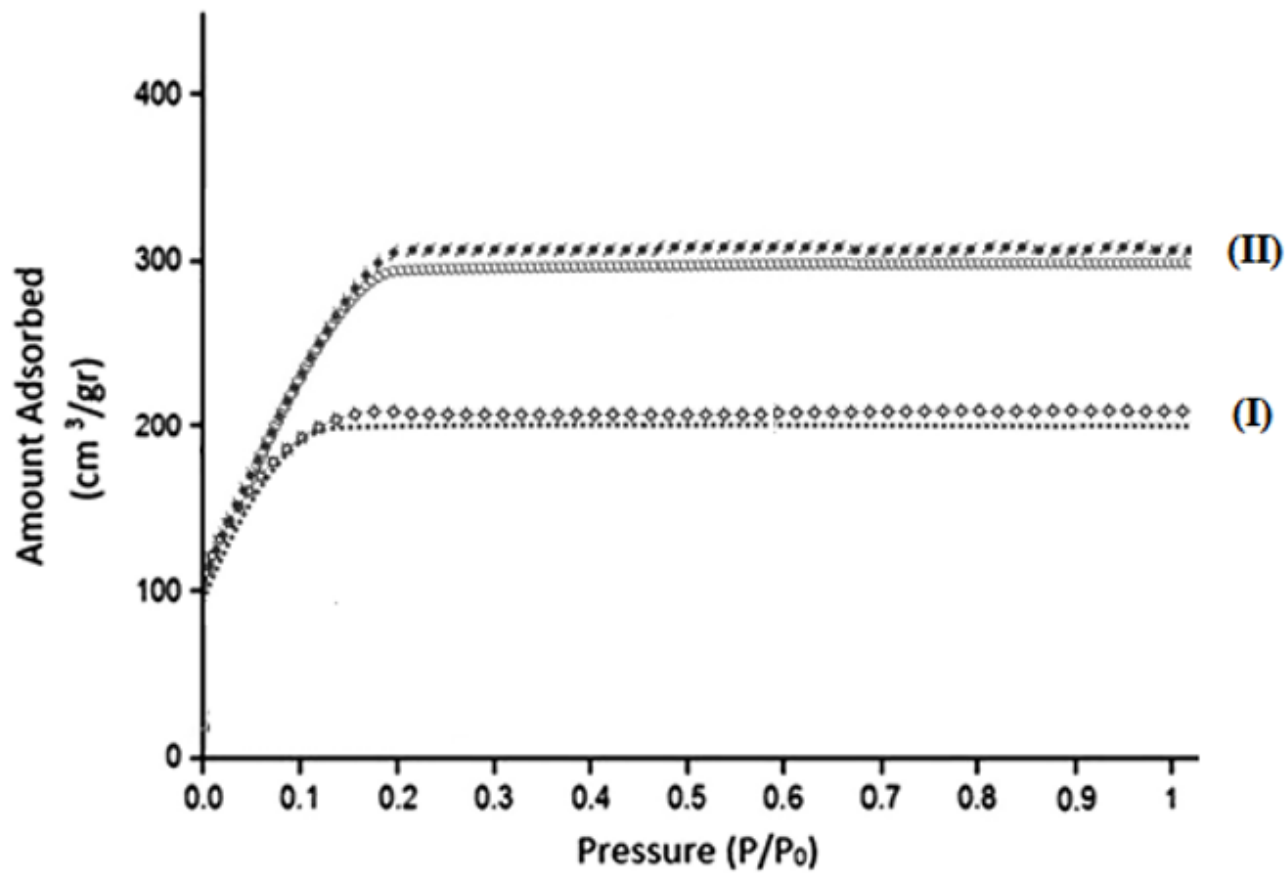


Figure 7

N₂ adsorption/desorption of Fe₃O₄@SiO₂ (I) and PVA/MFCP nanostructures (II)

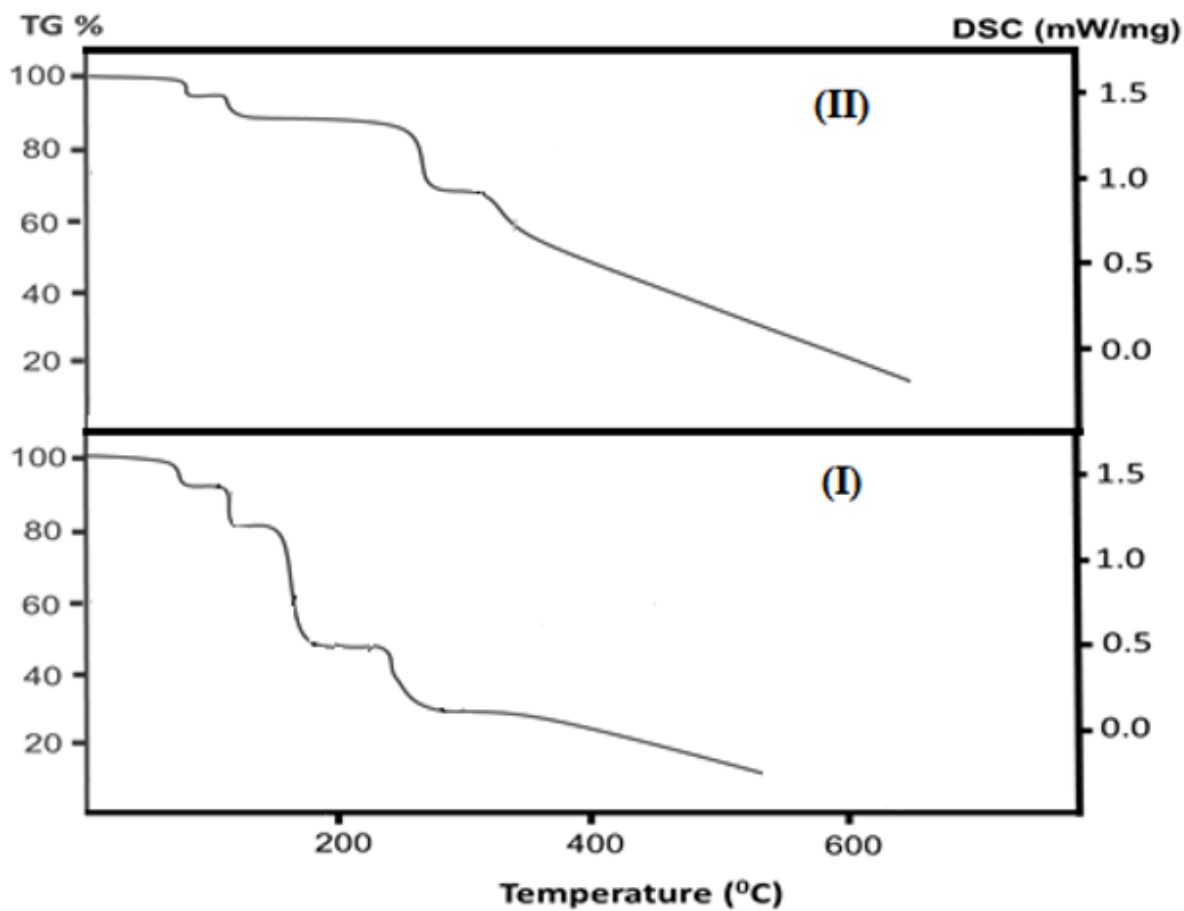


Figure 8

Thermal behaviour of $\text{Fe}_3\text{O}_4@\text{SiO}_2$ (I) and PVA/MFCP nanostructures (II)

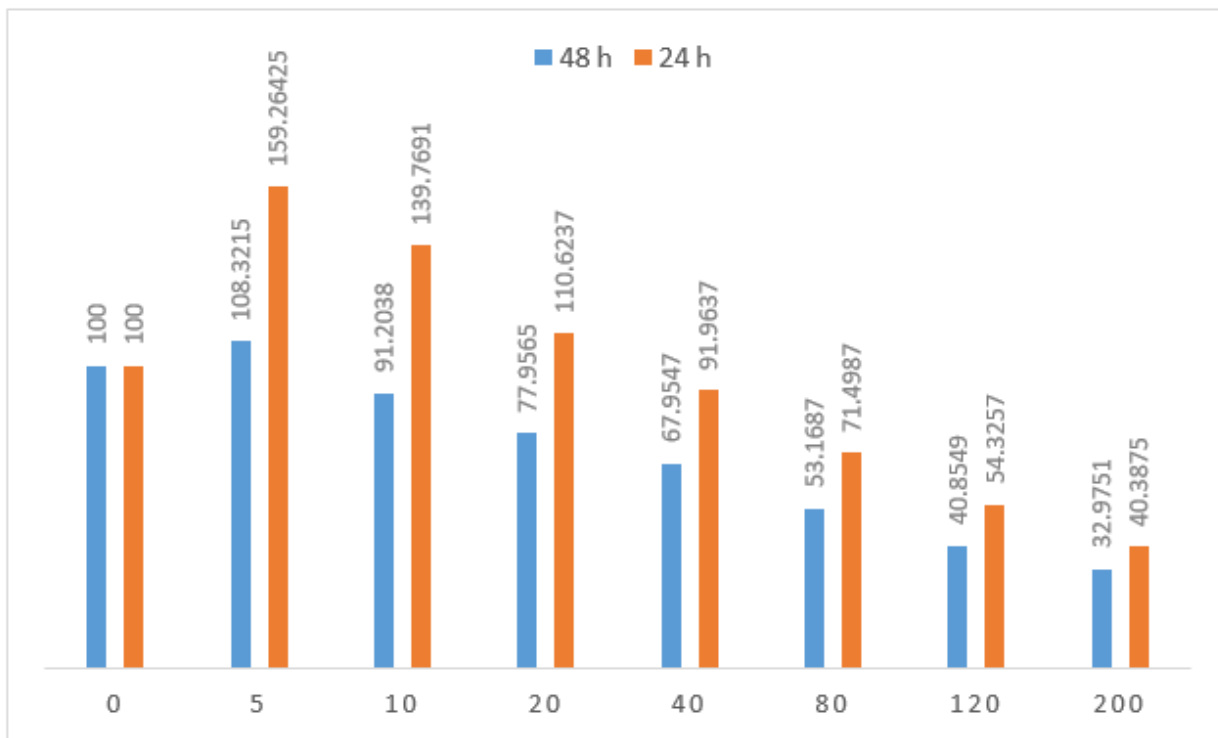


Figure 9

Anticancer activity of PVA/MFCP nanostructures on MCF-7 breast cancer cells